Sensors & Actuators: B. Chemical 300 (2019) 126963

Contents lists available at ScienceDirect

Sensors and Actuators B: Chemical

journal homepage: www.elsevier.com/locate/snb

Effect of receptor attachment on sensitivity of label free microcantilever based biosensor using malachite green aptamer

Yue Zhao, Agnivo Gosai, Pranav Shrotriya*

Department of Mechanical Engineering, Iowa State University, Ames, IA 50011, USA

ARTICLE INFO

Keywords:
Microcantilever
Aptamer
Malachite green
Laser interferometer
Sensitivity
Optical biosensor

ABSTRACT

Biosensors are often limited by lesser signal/noise ratio in the detection of low concentration target analyte which may be improved by modifying receptor configuration on the transducer. In this study, we report the improvement in sensitivity, through an increment in surface stress signal, due to the attachment/functionalization of malachite green aptamers with double thiolated ends on microcantilever based sensors, compared to the conventional single thiolated aptamers. Malachite green is deemed to be carcinogenic to humans and its detection using biosensors has been studied by many researchers. Our approach resulted in one order of magnitude improvement in the detection limit for malachite green, on the same sensor. The improvement is attributed to configurational changes of the aptamer on the cantilever surface, induced by the double thiolated attachment, which results in better propagation of mechanical response upon binding with the target malachite green, resulting in higher signal.

1. Introduction

Microcantilever (MC) based sensors [1,2] are widely studied for their capability of sensitive detection of biological/chemical species wherein the biological/chemical reactions on the transducer i.e. the microcantilever (MC) are transduced into mechanical signals (e.g. bending of MC [3,4], shift in resonant frequency [5], piezoresistance change [6]) which can be readily monitored using optical methods and other schemes [1,2,7]. The surfaces of the microcantilevers are coated with a thin film of receptor molecules which can react with target analyte molecules with certain sensitivity and specificity. In many cases, the analyte molecules can be detected by observation of the cantilever deflection [8,9], resulting in surface stress, due to the binding of target molecules on the functionalized surfaces of the sensors.

Thundat and his colleagues [10], first reported their findings on the Atomic Force Microscope (AFM) cantilever deflection due to changes of relative humidity, which revealed the potential of the AFM cantilevers to work as chemical and biological sensors. They also confirmed the detection of mercury adsorption on cantilever with picogram resolution [5,10]. Following this, several applications have been studied based on the micro-cantilever based sensors. Fritz et al. [11] observed MC deflection induced by the hybridization of single stranded, 12 nucleotide DNA (ssDNA) with different concentrations of the complementary ssDNA molecules. Since these initial reports, different applications have been developed for sensing various targets including chemicals/gases/drug molecules [1,12,13], explosives [14–16], DNA oligonucleotides [11,17–24], biomolecules [7,23,25–27], toxins [9,28] and biomarkers for sensors towards disease detection [6,8,29–32].

Theoretical studies and simulations were also conducted to explore the mechanism of MC deflection. Fritz et al. [2] hypothesized that the cantilever deflection in case of DNA hybridization is induced by two competing mechanisms: electrostatic repulsion between negative charges on the DNA strands and relaxation of steric hindrance as disordered ssDNA transition to ordered DNA strands. Mertens et al. [33], conducted experiments and proved that hydration forces are also major sources of the deflections besides electrostatic repulsions. With these assumptions, Strey et al. [34], established a liquid crystal model to investigate the pairwise potentials between hybridized DNA molecules on the cantilever surface, and showed that the hydration forces and electrostatic interactions have the dominant contributions to the surface stress changes, and the strengths of the pairwise potentials depend on the salt concentration and drops exponentially with the corresponding decay lengths. The dependence of MC deflection, due to DNA hybridization, on different distributions of DNA molecules on the MC surface has also been reported [3], and computational results considering randomly immobilized DNA molecules on MC surface [3], were in closer agreement to experimental reports [11,17,23], over

* Corresponding author at: 2019 Black Engineering Building, Ames, IA 50011, USA.
E-mail address: shrotriy@iastate.edu (P. Shrotriya).

https://doi.org/10.1016/j.snb.2019.126963
Received 17 April 2019; Received in revised form 8 August 2019; Accepted 8 August 2019
Available online 09 August 2019
0925-4005/

ordered arrangements like the hexagonal form. Tan et al. [35] have theoretically shown that elastic modulus of cantilever substrate has influence on the surface stress/deflection as well. Thus, it is possible to influence the signal of MC based sensors by developing a thorough understanding of the interaction between the DNA receptors/ligands on MC surface.

Unlike sensors for detection of chemicals/gas molecules [36,37], the sensors developed for detecting biological species like proteins and antigens, often suffer from low sensitivity and low detection thresholds [38], because in case of microcantilever biosensors, the deflection magnitudes and surface stress changes are often low during the binding of smaller concentration of target analyte, resulting in lesser signal to noise ratio. For example, surface stress changes of approximately 2–40 mN/m have been reported for hybridization of 9-mer to 30-mer ssDNA oligonucleotides [4,11,17,22,23,39]. The typical noise, in buffer, reported in laser interferometry based MC sensors, developed by our group, is less than 3 mN/m [13], and this could worsen in presence of interfering molecules available in complex sample like serum. Thus, low magnitude of signal consequently limits the sensitivity and detection limit associated with target analyte. Hence, the low sensitivity becomes an obstacle for MC based sensors for biological species detection in complex matrices [38]. Many attempts have been made to improve the threshold sensitivity of the sensing platform in biosensors like controlling sensing environments through manipulation of hydration [33,40], utilizing background protein to saturate non-specific interactions [41], adding new materials like magnetic beads [42], or proposing new structural arrangements of the receptor using 3-D DNA nanostructures [43]. In this study we propose a functionalization method to increase the sensitivity of an aptamer based microcantilever sensor to detect malachite green.

Malachite green (MG) is a triphenylmethane dye and was once widely used as an antiparasitic, antifungal and antimicrobial agent in agriculture/pisciculture [44]. Since the last two decades several studies have analyzed the detrimental effects of MG on the human health and environment and found it to be carcinogenic/mutagenic [45]. Despite the ban/stringent regulation on MG in several countries, it is still used illegally due to its low cost and efficiency. Hence, detection of MG, even in trace amounts, has assumed a major area of research. Different approaches utilizing techniques like electrochemical methods [46], fluorescent resonance energy transfer [47] and receptors ranging from antibodies [48], oligonucleotides [49], quantum dots [50] to molecularly imprinted polymers [47] have been reported.

Aptamers (short oligonucleotides, DNA/RNA) have been shown to change configuration upon binding with ligand [51] or due to external stimulus like change in pH and temperature [52], or electric field [53,54]. Aptamers are being increasingly used as receptors to detect biological elements like antigens and small molecules and even ions [51]. Aptamers can retain their functional properties over a wide variation of temperature, pH and other environmental factors and thus hold a lot of promise in the field of diagnostics. In this work, we report the investigation on the difference of surface stress changes due to various functionalization methods, which in turn can impact configuration, for thiolated malachite green aptamers (MGA). The combination of malachite green (MG) and MGA has been used to study RNAs in live cells [55] and the binding of MGA to MG increases the latter's fluorescence, which has important applications in cellular imaging studies. The MGA is chosen as the receptor in present work, as it undergoes a conformational switch upon binding with its target analyte, malachite green (MG), [56] and as reported earlier [3] and discussed in the previous paragraphs, the configurational arrangement of oligonucleotides on the MC surface has strong bearing on the surface stress, thus making the MGA an ideal candidate to investigate such effects. The different functionalization schemes are schematically illustrated in Fig. 1.

We consider two cases: (1) single thiolated and (2) double thiolated aptamers and look at how these two cases influence the sensitivity of a biosensor. The target analyte in this case is malachite green (MG) and surface stress changes are analyzed by a laser interferometry based microcantilever surface stress sensor. The surface density of aptamer for the different functionalization methods are also determined based on the fluorescent behavior of MG. Double thiolated aptamers are used to promote the configuration that is most conducive to binding with MG while bringing the structure closer to the microcantilever surface. According to our hypothesis, this would result in higher signal strength and better binding efficiencies. Through the research described in this work, we intend to establish double thiolation as a possibly viable technique to generate higher surface stress changes, accompanied by a concomitant increase in sensor signal, for lower concentrations of analyte, as compared to the straightforward single thiolated method.

2. Materials and methods

2.1. MGA/MG binding pairs

The malachite green aptamers (MGA) are short single-stranded RNA molecules which bind specifically to malachite green (MG) molecules. Structural analyses of the MGA/MG binding pairs [56,57] show that the aptamers have a tertiary structure and form a binding pocket for the MG molecules to sit inside and get locked. The MGA and MG molecules both change their structures during binding. To be specific, the MG molecule becomes flatter and the MGA develops twists in structure [56–58].

The thiolated MGA oligonucleotides were synthesized by Integrated DNA Technologies, Inc. (Coralville, IA) with the reported sequence [59] as listed: thiol-5′-GGA UCC CGA CUG GCG AGA GCC AGG UAA CGA AUG GAU CC-3′ (- thiol) (The second thiol group is optional for different experiment preparation). MG molecules were purchased from Sigma (St. Louis, MO). The IDT Oligoanalyzer program was utilized to review the secondary structure of the double thiolated aptamer and the results are given in Figs. 5 & 6 of the Supplementary information. The predicted structures suggest that both of the double thiolated groups should be in the same orientation and thus facilitate attachment to the gold surface of the microcantilever.

2.2. Micro-cantilever specification and sensor preparation

High aspect ratio tipless AFM cantilevers used in the sensor system were purchased from Nanoworld, Switzerland. The cantilevers used were 500 μm long, 20 μm wide and 1 μm thick, and coated with 5 nm of titanium and 30 nm of gold film. In the sensor system, a sensing/reference pair of MCs were used. The sensing cantilever was immobilized with the thiolated MGA molecules and the reference cantilever was immobilized with scrambled RNA, of equal nucleotide length, that has very less affinity to the target MG molecules. The scrambled oligonucleotide sequence on the reference cantilever is: thiol-5′-GGG GAG ACA AGA AUA AAC GCU CAA UUC GAC A GG AGG CU-3′-thiol, as per the control nucleotide described in Wang et al.'s study [56]. Two distinct types of sensing MCs were prepared, one functionalized with MGA with one thiol group at 5′ end, and the other functionalized with MGA with thiol groups at both 3′ and 5′ ends.

2.3. Differential interferometer

The microcantilever (MC) based detection system (Fig. 2) incorporates a differential surface stress measuring interferometer having a sensing/reference MC pair. A brief description of the working principle is provided in this article, and readers are encouraged to consider previous studies [13,20,60], by our group for a detailed explanation. Measurement of differential surface stress ensures that the detected signal is proportional to the specific binding of target analyte to the aptamer functionalized sensing MC only, due to the elimination of the influence of ambient disturbances/noise sources such as nonspecific

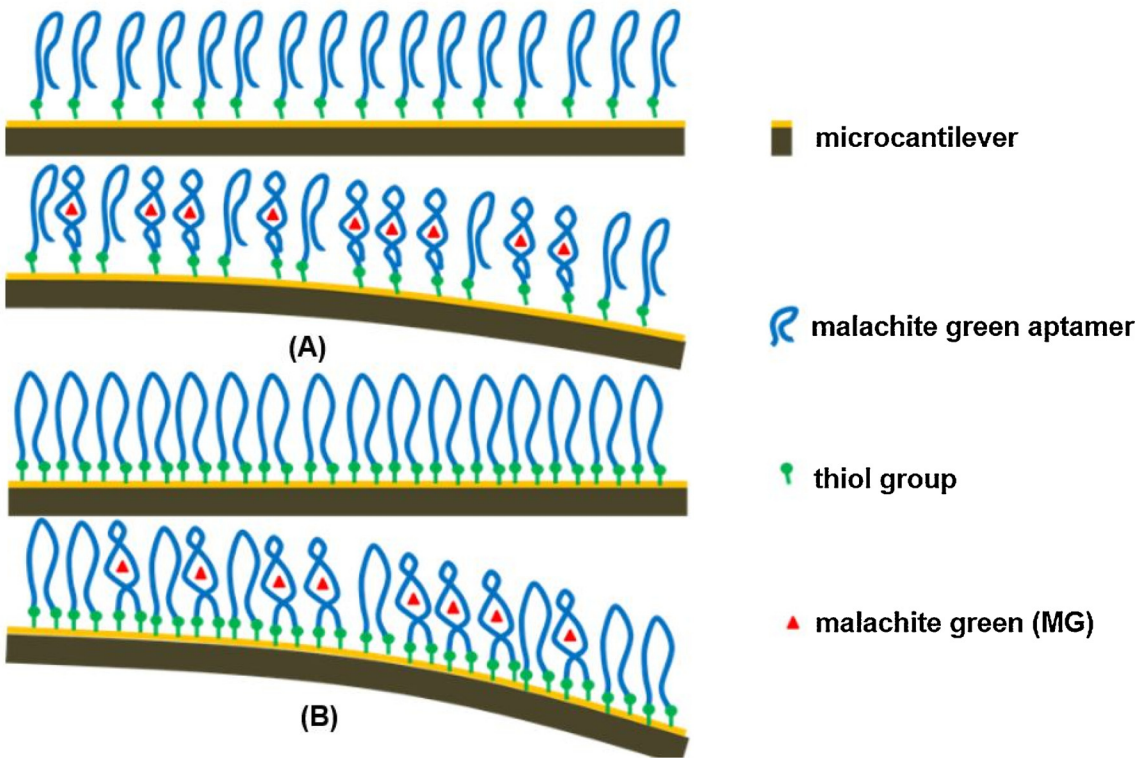

Fig. 1. Schematic illustration of different immobilization methods. (A) Single thiolated MGA immobilization; (B) Double thiolated MGA immobilization.

binding, changes in pH, ionic strength, and especially the temperature, as a result of having the reference MC. In the scheme shown in Fig. 2, two laser beams of mutually orthogonal polarizations were generated using the calcite beam displacer and they are let to shine on the sensing and reference cantilevers.

Upon reflecting from the cantilevers and passing through the beam displacer, the beams are recombined into one and become an elliptically polarized beam whose two linear components have a path length difference equal to twice the differential displacement (Δl) between the cantilevers [61]. This single light beam was collected and interfered, utilizing the Walloston positioned at 45° relative to the merged reflective beam, and the intensities of the two interfered fringe patterns were monitored through the two photodiodes. The optical signals were thus converted to electrical signals, I_1 and I_2, by the two photodiodes. The photodiodes signals may be represented as follows:

$$I_1 = \frac{1}{4}[I_s + I_r + 2\sqrt{I_s I_r}\cos\varphi],\ I_2 = \frac{1}{4}[I_s + I_r - 2\sqrt{I_s I_r}\cos\varphi] \quad (1)$$

where, I_s, I_r are the light intensities of the reflected beams from sensing and reference MC respectively, φ is the phase difference between the

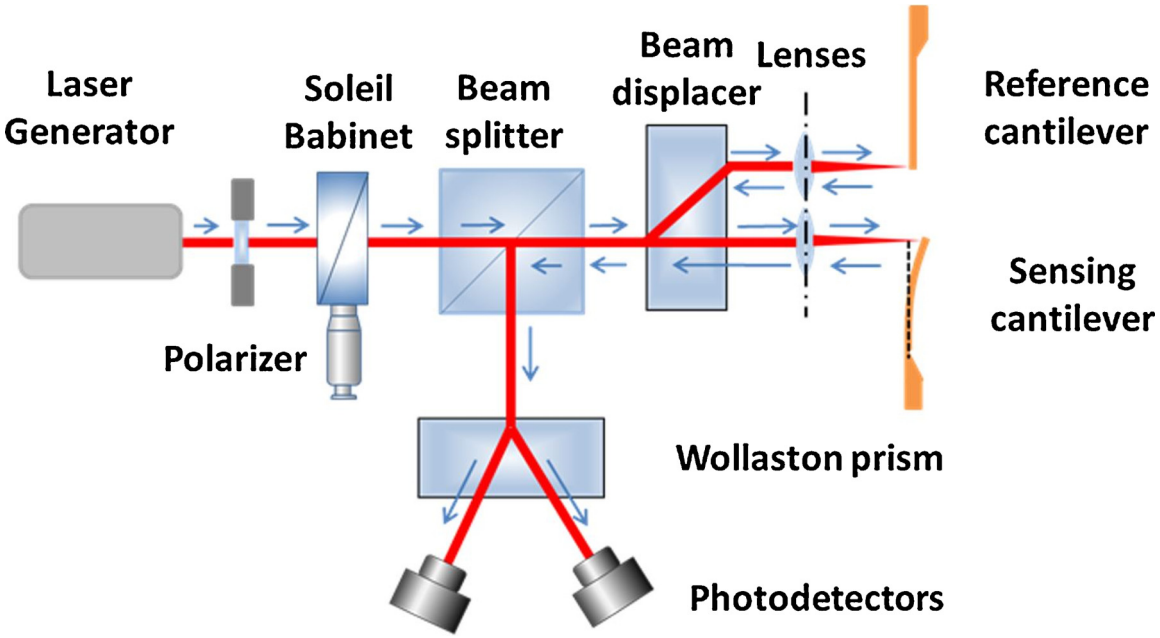

Fig. 2. Schematic layout of differential surface stress based laser interferometer.

reflected beams [60]. As a result, we can monitor the change of the phase difference between the reference and sensing beams as follows:

$$\cos\varphi = A\frac{I_1 - I_2}{I_1 + I_2},\ A = \frac{(I_s + I_r)}{2\sqrt{I_s I_r}} \quad (2)$$

When the MG solution was introduced to the cantilever pair, a differential surface stress change was generated during binding, and a differential cantilever deflection Δl was induced. As a result, the path length difference travelled by the two reflected laser beams were shifted by a value of $2\Delta l$, and the corresponding phase difference of $\varphi = 2\Delta l/\lambda$ was observed, where λ is wavelength of the laser (635 nm). The intensity of the interfered fringe was monitored and recorded during the whole procedure of MG introduction till the signal achieved stability. By analyzing the interfered signal, the differential deflections could be calculated as $\Delta l = \lambda\Delta\varphi/4\pi$. Finally, the surface stress change Δσ is given by Stoney's equation [61]:

$$\Delta\sigma = \frac{E}{3(1-\nu)}\left(\frac{t}{L}\right)^2(2\Delta l) \quad (3)$$

where E is the elastic modulus, ν is Poisson's ratio, L is the length, and t is thickness of the microcantilevers.

2.4. Microcantilever functionalization

In preparation of the experiments, all the MC were cleaned with piranha solution (70% H_2SO_4 and 30% H_2O_2) for 1 min and then rinsed in deionized water. The thiolated MGA were diluted to 0.5 µM concentration with the immobilization buffer (50 mM Tris-HCl, 150 mM NaCl, 5 mM $MgCl_2$, pH 7.4), and heated up to 90 °C followed by cooling to room temperature for refolding the aptamer. The sensing MCs were immersed in the MGA solution for 3 h to allow functionalization, followed by washing in immobilization buffer to remove non-specifically bound aptamers. The sensing MCs were then treated with 3 mM 6-mercapto-1-hexanol (MCH) solution to block any vacant gold surface. Herne et al. [62] were amongst the first group to demonstrate the efficacy of using a mixed monolayer of MCH and ssDNA on gold surfaces. That study along with the experiments reported by Levicky et al. [63] and Keighley et al. [64], showed that MCH blocked non-specific contacts between the DNA backbone and the gold surface, displaced weakly adsorbed DNAs and the mixed monolayer could achieve nearly 100% binding efficiency to target analytes. MCH has been previously used as passivating agent in several biosensor studies, for e.g. on electrochemical biosensor transducer surfaces for detection of thrombin [65] and small molecule like doxorubicin [41] including microcantilever based biosensors to detect cocaine [13] and cancer biomarker nucleolin [8] and no detrimental effects are widely reported. The reference cantilever was also passivated with MCH in the same procedure, where the MGA had been replaced by the scrambled oligonucleotide.

2.5. Surface coverage density tests

Before the surface stress experiments were conducted with the sensor, the coverage densities of the sensing cantilevers for both of the single and double thiolated MGA were determined with fluorescence tests following the method outlined by Demers et al. [66]. After the functionalization of the sensing cantilever with the MGA, it was merged in the etching/removing buffer (12 mM β-mercapthoethanol) for 48 h to remove the aptamer. The MGA molecules attached on the MC surface were removed and released into the buffer during the procedure and the same buffer was used to complete the fluorescence tests based on the fluorescent behavior of MG. Details are provided in Supplementary information.

2.6. Surface stress experiments

The sensing experiments were carried out for both single- and double thiolated aptamer scenarios with different concentrations of MG in the binding buffer (10 mM HEPES, 100 mM KCl, 5 mM $MgCl_2$, pH 6.0). The pH value was chosen for the particular MG aptamer to promote maximum binding to MG molecules, in accordance to previous reports [56]. The sensing and reference microcantilevers were mounted in the interferometer system and submerged in the binding buffer. The MG solution was introduced to the experimental chamber in the laser interferometer system and the interfered signals were monitored during the differential deflection development. All experiments were conducted at an average room temperature of 25 °C.

Three different sets of experiments were carried out with three distinct types of sensing MCs: (1) MC functionalized with single thiolated MGA; (2) MC functionalized with double thiolated MGA; and (3) MCs which were functionalized with the binding complex of double thiolated MGA and MG, and then washed with double distilled water having temperature of 80 °C to remove the MG molecules. Washing above the melting temperature of MGA affects its configuration and thus releases the binding with MG molecules.

3. Results

3.1. Surface coverage density

Three measurements were taken for both single- and double thiolated MGA functionalization. Fluorescence signal range was observed to be of similar magnitude for identical MG concentration in case of both single and double thiolated aptamers. The surface coverage densities were then found to be 0.057 ± 0.05 and 0.042 ± 0.04 molecules/nm^{-2} for single and double thiolated MGA respectively, with a 90% confidence interval, following the work by Demers et al [66]. Considering a hexagonal close packed arrangement, the separation distance between two neighboring aptamers are calculated as 4.5 and 5.2 nm for single and double thiolated MGA respectively. This possibly indicates that double thiolated MGA backbone could be brought closer to the microcantilever surface to accommodate the entire aptamer in the space which maintains almost equal inter-aptamer distance like the single thiolated functionalization scenario. The results are detailed out in the Supplementary information.

3.2. Surface stress change

The MC surface stress measurements were conducted with equal volume injections of MG solutions having different concentrations. Fig. 3 shows a typical profile of the surface stress development during the binding of MGA and MG molecules. The plot with 0 concentration of MG is due to buffer injection which provides the noise level (2 ± 1 mN/m). Surface stress changes developed after the injection of the MG solution into the system and reached the saturation state within 15–20 min on an average. For e.g., surface stress change of ˜20 mN/m was observed with single thiolated MGA for final MG concentration of 100 nM. The range of surface stress change for experiments involving set 1 with single thiolated MGA was 10–53 mN/m. For experiments involving set 2 with double thiolated MGA, the surface stress change was 9–70 mN/m, whereas that for experiments involving set 3 indicated a surface stress range of 14–85 mN/m. For all the different sets, the MG concentration range was 5–5000 nM MG solutions. These results are shown in Fig. 4(A) and (B). The details, including statistical calculations, are provided in Supplementary information.

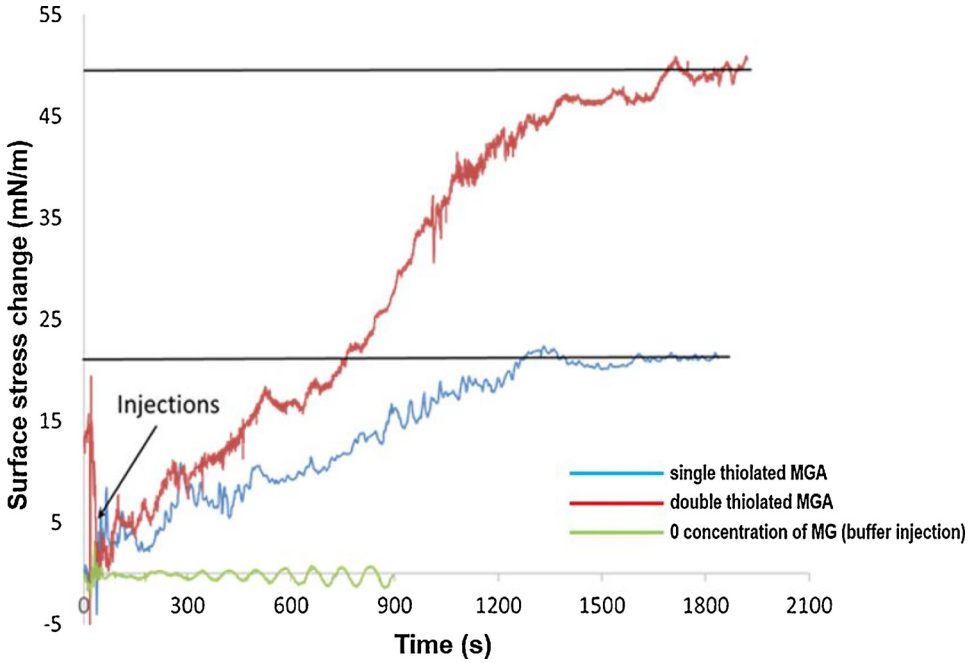

Fig. 3. Typical profile of surface stress development during MGA/MG binding with a concentration of 100 nM of MG in the experimental cell.

4. Discussion

4.1. Comparison between single and double thiolated aptamers

Surface coverage tests showed that the coverage densities for both single- and double thiolated MGA functionalization turned out to be of the same magnitude, in average 0.09 and 0.08 molecules/nm^{-2} respectively, for NaCl concentration of 150 mM. The results of surface coverage is in agreement with previous reports [22,67] for similar salt concentration and nucleotide length. In addition, the average separations between immobilized aptamer molecules were calculated to be 4.5 and 5.2 nm respectively for single and double thiolated cases, based on the hexagonal close packed assumption [3].

The surface stress measurements, which are the sensor response, associated with the binding of MGA and MG, on the three distinct sets of MCs, are plotted and compared in Fig. 4(A) and (B). The results show that, for the same MG concentration, the double thiolated cases resulted in higher surface stress changes than those of single thiolated cases, and experiments from Set-3 provided the highest surface stress change, at the saturation zone. At low concentrations, the double thiolated aptamers (sets 2 and 3) induced much greater surface stress changes, and the threshold detection limit was increased by about 10 times (from ~50 nM to ~5 nM). The detection limit was determined for the lowest MG i.e. target concentration which still provided signal to noise ratio (SNR) ~3. For e.g. for sets 2 and 3, the average signals at 5 nM of MG are ~12 and ~15 mN/m respectively, and for a maximum blank response of 3 mN/m (noise, due to buffer injection) the SNR ~4–5 and thus higher than the required value of 3. It is observed from Fig. 4(B) that for MG concentrations less than or equal to 100 nM, the sensor response for both sets 2 and 3 are mostly identical as signified by the strong overlap of the confidence intervals. However, the surface stress changes show saturation in maximum signal, at lower MG concentration, for the sets of experiments with double thiolated MGA (500 nM for set 2, 1000 nm for set 3) compared to the single thiolated MGA (~2000 nM for set 1).

The equilibrium reaction of the binding and the corresponding disassociation constant (k_d) are studied as well for the different cases. The experimental data for the three different cases are fit to the Langmuir isotherm equation (Sensor response $\propto = \frac{[Malachite\ \ green]}{[Malachite\ \ green]+k_d}$) to obtain an estimate of the k_d [41]. The fit (solid lines) along with the 95% confidence intervals (dashed lines), for the three cases, are shown in Fig. 4(A) and (B). Relative standard deviations (RSD) for the observed stress changes with respect to particular concentration of MG are reported in Supplementary Table S1. The k_d values for set-1 (single thiolated), set-2 (double thiolated) and set-3 (double thiolated MGA, which was previously bound to MG) are 179 ± 8 nM, 37 ± 11 nM and 45 ± 13 nM. The reduction of k_d by one order of magnitude from that in set-1 to the values in set-2 and set-3 may be attributed to molecular crowding effects [68], due to the different configurational aspect of doubly thiolated aptamer in comparison to single thiolated aptamer. Through experiments [41] and multiscale simulations [53], we have previously reported that thrombin aptamer attached to the sensor surface though a single thiol bond, has smaller k_d (0.5–1.2 nM) for its ligand thrombin, compared to the solution k_d of the complex (3–25 nM) [69]. Similar reduction in k_d is observed for the single thiolated aptamer-malachite green complex compared to its solution k_d of about 800 nM [56], and the k_d is further reduced by one order of magnitude for double thiolated aptamer (Table 1). Thus, it can be postulated that the configuration of aptamer on the surface has a significant role in its interaction with the ligand.

4.2. Surface stress change vs binding efficiency

According to previous reports [3], single thiolated DNAs have pairwise interactions which lead to a second order relationship between surface stress changes and hybridization efficiency. Here we assume that the efficiency of binding between MGA and MG molecules is a physical quantity which is similar to hybridization efficiency between the interacting single stranded nucleotides. This provides a relationship as follows:

$$\Delta\sigma = K\varphi^2 \tag{4}$$

where $\Delta\sigma$ is the surface stress change, φ = binding efficiency and K is the strength constant. The binding efficiency φ can be defined as:

$$\varphi = \frac{c}{c + k_d} \tag{5}$$

The surface binding efficiencies corresponding to each concentration can be calculated with the respective k_d value, and the surface stress changes were plotted with the binding efficiency or fraction of aptamer

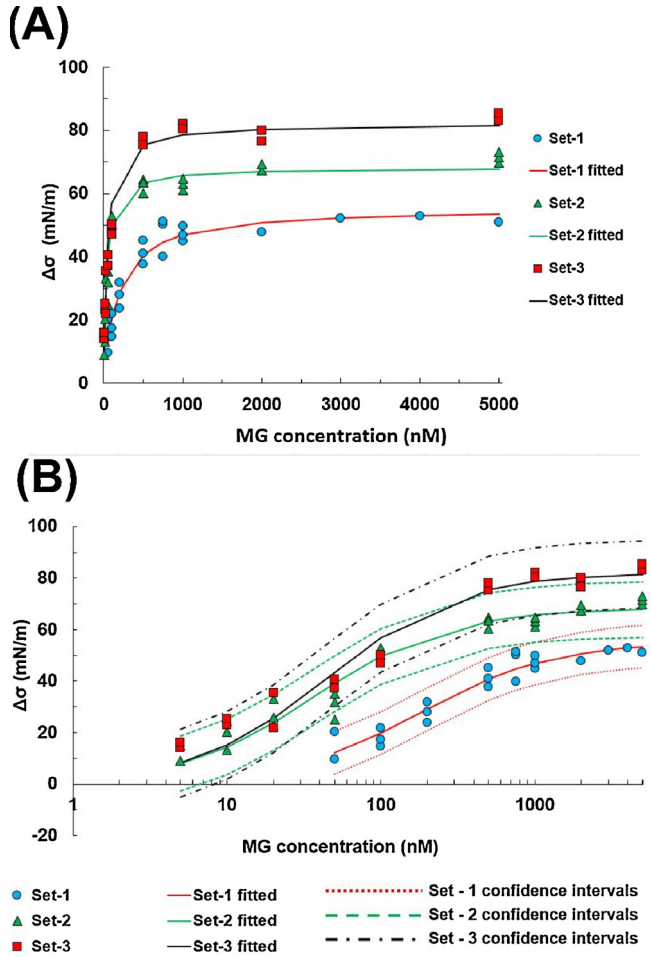

Fig. 4. (A) Surface stress change vs. MG concentration for 3 different immobilization methods. Set-1, Set-2 and Set-3 correspond to single thiolated, double thiolated and double thiolated aptamers which were previously bound to MG, respectively. The Langmuir isotherm fit for each of the data is given by the solid line (B) The concentration of MG is plotted in log scale to resolve the response due to concentrations lower than 100 nM. The 95% confidence intervals from the Langmuir fit, for each of the experimental sets are shown by dashed lines.

bound for all three sets of measurements in Fig. 5.

The results show that the relationship between surface stress change and binding efficiency for single thiolated case (set 1) was increasing non-linearly following Eq. (6). While for double thiolated cases (sets 2 and 3), the surface stress changes show a linear relationship with the binding efficiency, i.e. $\Delta\sigma \propto \varphi$ and sensitivities (signal change over analyte/target concentration, signified by the slope of the linear portion of the curves)are constant (˜64 and 75 mN/m nM respectively), which are 6–7 times of the sensitivity (˜11 mN/m nM) of set 1 at low binding efficiencies (less than 40%). Hence, the sensor shows greater sensitivity for low concentration of target in case of the double thiolated aptamers in contrast to the conventional single thiolated aptamers. It may be

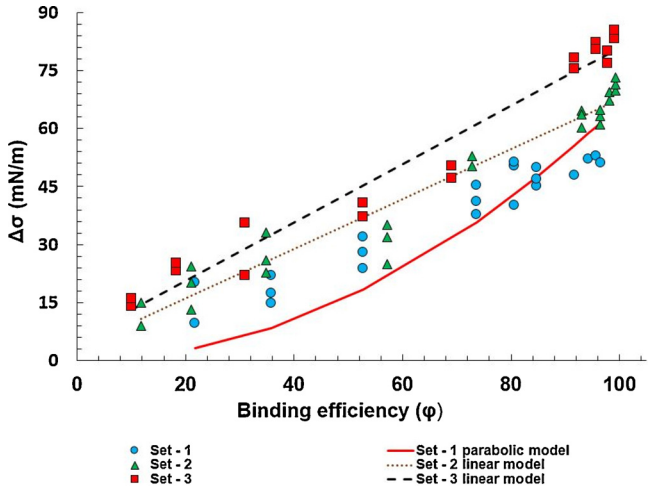

Fig. 5. Surface stress change vs binding efficiency for all 3 sets of measurements. Set-1, Set-2 and Set-3 correspond to single thiolated, double thiolated and double thiolated aptamers which were previously bound to MG, respectively.

observed that the set 1 does not truly follow the parabolic fit for lower binding efficiency ($\varphi < 40\%$), as the response is mostly linear in that regime. Similar linear response at lower analyte concentrations, for single thiolated aptamers on microcantilever sensors has been reported earlier by Kang et al. in the case of cocaine aptamers [13].

It is generally assumed that the surface stress change is induced by the pairwise potential due to the conformational change of the molecules after binding with the targets. The possible potentials include electrostatic repulsions due to deprotonation, conformational entropy along with repulsive steric interactions, and buffer-counterion osmotic pressure. Earlier studies showed that among all these interactions, the hydration forces due to disturbance on the hydrogen bonding network are the dominant factor for the surface stress generation [29,33,34], and simulations [3] based on that can reasonably predict the surface stress change for single thiolated case, and the magnitude depends on the surface coverage density or the inter-molecular separations. However, the surface coverage tests for the experiments described in the present study showed that the surface densities are similar for the different functionalization types (Supplementary information), which confirms that the differences in surface stress changes for different measurement sets are not dependent on surface coverage. Stress difference due to temperature fluctuations can also be ruled out as the experimental set-up utilizes a pair of sensing-reference microcantilevers for elimination of environmental disturbances [20,21]. As a result, the surface stress changes with double thiolated sets (sets 2 and 3) were assumed to be due to some other factors. From the surface coverage measurements (Supplementary information) it is observed that the inter-molecular distances between two MGA molecules are of comparable magnitude for both the single as well as double thiolated aptamers. Since the double thiolated functionalization will attach both ends of MGA onto the surface of the cantilever, the backbone of the aptamers are pulled closer to the surface.

The electrostatic effects resulting from the molecular

Table 1
Sensor parameters for the different sets of experiments.

Case	Lower limit of detection (nM)	Signal saturation concentration (nM)	Linear range of detection (nM)	Sensitivity in linear range (mN/m. nM)	k_d calculated from Langmuir fit (nM)
Set-1 – single thiolated MGA	50	˜2000	˜1950	11 (for $\varphi < 40$ %)	179 ± 8
Set-2 – double thiolated MGA	5	˜500	˜495	64	37 ± 11
Set-3 – double thiolated MGA which were previously bound to MG	5	˜1000	˜995	75	45 ± 13

Table 2
Comparison with other techniques/methods.

Method/Technique	Receptor	Transducer	Detection Limit (nM)	Remarks	Reference
Electrochemical	Aptamer	Glassy Carbon Electrode	3.38	Electrode modified with gold nanoparticles, graphen quantum dots - tungsten disulphide	Wang et al. [46]
Piezoresisitve/tively.Tsuface stress	G-Telomere DNA	carbon black-SU8-glycidol piezoresistive microcantilver	100	G-quadruplex formation produces signal	Vinchurkar et al. [75]
Electrochemical	NA	Glassy carbon electrode	100	Electrode modified with graphene quantum dots/gold nanoparticles; Detection performed in fish sample	Hou et al. [76]
Electrochemical	NA	carbon nanohorns and alkoxy modified glassy carbon electrode	81.9	Detection demonstrated in fishery water	Dai et al. [77]
Electrochemiluminescence	Aptamer	CdS quantum dots modified screen printed electrode	0.03	Hybridized aptamer is released to produce signal on binding with MG	Feng et al. [50]
Fluorescence resonance energy transfer	Molecularly imprinted polymer	CdTe quantum dots	59	Detection demonstrated in spiked fish sample	Wu eta al. [47]
ELISA	Polyclonal antibody - enzyme	Microwell	0.3	Detection demonstrated in fish sample; a derivative of malachite green was synthesized to prepare the antigen	Xing et al. [48]
LC-MS	NA	NA	0.09	Detection was performed in water	Mitrowska et al. [73]
SERS	NA	NA	1.5	Detection was demonstrated in fish muscle tissue sample; gold nanoparticles utilized	Zhang et al. [74]
Laser interferometry	Aptamer	Gold coated microcantilever	5	Aptamers thiolated at both 5' and 3' ends increased sensitivity and improved LOD	This work

NA = Not applicable.

conformational change upon binding with target could have greater influence on the gold coated sensing surface of the microcantilever. The isoelectric point of MG molecules is 3.0 [49], and the experimental buffer pH of 6.0 ensures an overall negative charge for the MG molecule. The aptamer is also a negatively charged molecule due to the phosphate groups on the RNA. The change in configurational distribution of negative charges, over the microcantilever surface, owing to the change in aptamer configuration due to double thiolation, in contrast to the single thiolated case may result in the surface stress difference. The conformational changes of the MGA before and after binding with the MG have been studied previously by Flinders et al. [70] and Wang et al. [56] and it was observed that the MGA molecules will have a significant twisting on the molecular structure. Particularly Flinders et al. [70], noted that intramolecular interactions within the aptamer folds the phosphate backbone in a structure that results in an asymmetric distribution of charge within the binding pocket that also forces the ligand i.e. MG molecules to undergo a partial redistribution of charge [57]. It could be that the resultant forces due to such interactions may transmit to the sensing/transducer surface, much effectively due to double thiolation which brings the aptamer closer to microcantilever surface as the inter-aptamer distance is almost equal to that of the single thiolated case (Supplementary information). Thus, the microcantilever surface will suffer greater reconstructions, which would possibly lead to larger cantilever deflections, and result in an increased surface stress signal and higher sensitivity. It is interesting to note that recently Zhang et al. have also attributed the surface stress signal in their version of microcantilever based biosensor to the structural switching of a cyanotoxin aptamer upon binding with its target [71].

There is also the possibility of improved binding with MG molecules as a result of the double thiolation which can promote favorable configurational arrangement by exposing the aptamer binding pocket in a favorable orientation while bringing the aptamer closer to the microcantilever surface. Bernard et al. [72] have reported that MGA recognizes and binds to its target i.e. MG mainly via π-π stacking as well as electrostatic interactions. The π–π stacking stabilizes the non-covalent interactions that are a common occurrence for interactions involving parallel aromatic rings [73]. Certain base pairs on the aptamer serve as stacking platforms for its target whereas neighboring base pairs act as anchors/linkers facilitating the binding process. Similar interactions are also reported by Wang et al. [56], where they also showed that proper orientation of aptamer enables greater binding efficiency and a lower k_d.

Although the lower limit of detection was improved by one order of magnitude, the signal saturation concentration was brought down to 500 nM (set 2) from 2000 nM (set 1), which reduces the linear range (Table 1). We propose that the double thiolated MGA from set 2 of the experiments promote conducive configuration for binding to MG and only a small fraction of the aptamers would be restricted to configurations which need more instances to bind with MG as could be the case for the single thiolated aptamers of set 1. This may explain the improvement in k_d from ˜179 to ˜37 Nm. Set 3 was designed to improve this further by immobilizing the surface with MGA molecules which were previously bound with MG, to possibly retain the most favorable binding configuration of the aptamer. It could be conjectured that this was made primarily possible by constraining free movement of the oligonucleotide as both ends of the aptamer were tethered to the microcantilever surface previously. In this manner, most MGA molecules attached to the surface were supposed to retain the configuration/structure amenable to binding with MG. The measurements showed that the saturation concentration was raised to 1000 nM with set 3, thus improving the dynamic range over that of set 2. However, at present a proper mechanism for this variation in dynamic range between sets 2 and 3 could not be derived. The results are provided in Table 1.

4.3. Comparison with other techniques

Several researchers have studied malachite green detection and a selection of these efforts are mentioned in Table 2. Electrochemical techniques utilizing nanomaterials modified glassy carbon electrodes could achieve a detection limit of 82–100 nM in contaminated fishery water/fish samples. Whereas the utilization of quantum dots and gold nanoparticles on aptamer receptors could achieve ultra-low detection of 0.03 nM. Well established detection methods like liquid-chromatography mass-spectrometry (LC–MS) [74] and enzyme linked immunesorbent assay (ELISA) [48] as well as surface enhanced Raman spectroscopy [75] involve sophisticated instrumentation and many pretreatment processes. In that regards electrochemical methods have an advantage of being comparatively cheaper but may involve the utilization of different nanomaterials to enhance the sensitivity and take advantage of labeling of biomolecules. The present work provides an alternative technology based on an optical method like laser interferometry for the label-free detection of MG using aptamers, minimum process steps and reagents. The time required to achieve a saturated signal is in the order of 30 min (Fig. 2). Also, laser interferometers can be made from fiber-optic components to reduce the equipment footprint and combined with chip-based analyzers to provide a compact solution. Still further studies are required to check their cost competitiveness with electrochemical methods. As per Culp et al. [45], MG exists as leuco-malachite green in fish tissue at an average concentration of ˜15 nM, which is within the detection range (LOD ˜ 5 nM) of the method described in this work. One limitation of this study is that the effectiveness of double thiolated aptamers were not tested in presence of interfering molecules which will be present in samples collected from fisheries etc., even though the aptamer has been selected [46,59] against possible cross reacting agents.

5. Conclusion

In the present work, a new functionalization method has been described and tested to achieve the goal of improving the performance of microcantilever based biosensors. Instead of having thiol groups on one end of the MGA molecules (receptor), used to attach the receptors to the microcantilever surface, they were functionalized with thiol groups on both ends of the aptamer. The new technique is demonstrated in the detection of malachite green, which is a small molecule of importance in aquaculture, molecular imaging and is being considered as a health hazard as well. Experimental results showed that the double thiolated functionalization method for the aptamer can increase the sensitivity for lower concentrations and improved the threshold detection limit by one order of magnitude.

It was noticed that the surface coverage density measurements of MGA showed similar surface densities for both the single as well as the double thiolated aptamers. Therefore, the enhanced response of the sensor could be due to interactions induced by the double thiolated MGA configuration on the surface which promotes increased binding efficiency with MG. Reports on MGA structure studies have shown that MGA molecules twist when bound with MG, and the configurational proximity of the double thiolated aptamer to the cantilever surface may translate to higher surface stresses. Therefore, the new functionalization method tends to induce stronger surface reconstructions on the sensor and lead to greater surface stress changes.

One side effect of the double thiolated functionalization is that the dynamic/linear range of detection is reduced. An adjustment is conducted to mitigate this side effect by functionalization with double thiolated MGA which were previously bound with MG. This was done to promote the configuration that is most favorable for the aptamer to bind with its target. However, the mechanism behind this improvement in dynamic range is not clearly understood. Other receptor-target combinations, as well as response of the sensor in complex matrices involving interfering molecules, need to be tested to prove the validity and utility of the double thiolated approach as a universal technique.

Declaration of Competing Interest

The authors declare no competing financial interests.

Acknowledgements

The authors gratefully acknowledge helpful discussions and suggestions from Prof. Marit Nilsen-Hamilton, Iowa State University. Yue Zhao and Pranav Shrotriya were partially supported on NSF (USA) career development grant CAREER CMMI-0547280. The authors would also like to thank the anonymous reviewers for their suggestions in improving the article.

Appendix A. Supplementary data

Supplementary material related to this article can be found, in the online version, at doi:https://doi.org/10.1016/j.snb.2019.126963.

References

[1] N.V. Lavrik, M.J. Sepaniak, P.G. Datskos, Cantilever transducers as a platform for chemical and biological sensors, Rev. Sci. Instrum. 75 (July (7)) (2004) 2229–2253.
[2] J. Fritz, Cantilever biosensors, Analyst 133 (7) (2008) 855–863.
[3] Y. Zhao, B. Ganapathysubramanian, P. Shrotriya, Cantilever deflection associated with hybridization of monomolecular DNA film, J. Appl. Phys. 111 (April (7)) (2012).
[4] S.L. Biswal, D. Raorane, A. Chaiken, et al., Nanomechanical detection of DNA melting on microcantilever surfaces, Anal. Chem. 78 (October (20)) (2006) 7104–7109.
[5] T. Thundat, E.A. Wachter, S.L. Sharp, et al., Detection of mercury-vapor using resonating microcantilevers, Appl. Phys. Lett. 66 (March (13)) (1995) 1695–1697.
[6] H.H. Kim, H.J. Jeon, H.K. Cho, et al., Highly sensitive microcantilever biosensors with enhanced sensitivity for detection of human papilloma virus infection, Sens. Actuators B: Chem. 221 (2015) 1372–1383 2015/12/31/.
[7] Y. Arntz, J.D. Seelig, H.P. Lang, et al., Label-free protein assay based on a nanomechanical cantilever array, Nanotechnology 14 (January (1)) (2003) 86–90.
[8] H. Li, X. Bai, N. Wang, et al., Aptamer-based microcantilever biosensor for ultrasensitive detection of tumor marker nucleolin, Talanta 146 (2016) 727–731 2016/01/01/.
[9] X. Zhou, S. Wu, H. Liu, et al., Nanomechanical label-free detection of aflatoxin B1 using a microcantilever, Sens. Actuators B: Chem. 226 (2016) 24–29 2016/04/01/.
[10] T. Thundat, R.J. Warmack, G.Y. Chen, et al., Thermal and ambient-induced deflections of scanning force microscope cantilevers, Appl. Phys. Lett. 64 (May (21)) (1994) 2894–2896.
[11] J. Fritz, M.K. Baller, H.P. Lang, et al., Stress at the solid-liquid interface of self-assembled monolayers on gold investigated with a nanomechanical sensor, Langmuir 16 (December (25)) (2000) 9694–9696.
[12] J. Tamayo, A.D.L. Humphris, A.M. Malloy, et al., Chemical sensors and biosensors in liquid environment based on microcantilevers with amplified quality factor, Ultramicroscopy 86 (January (1–2)) (2001) 167–173.
[13] K. Kang, A. Sachan, M. Nilsen-Hamilton, et al., Aptamer functionalized microcantilever sensors for cocaine detection, Langmuir 27 (December (23)) (2011) 14696–14702.
[14] V. Seena, A. Rajoriya, A. Fernandes, et al., Fabrication and characterization of novel polymer composite microcantilever sensors for explosive detection, MEMS 2010: 23rd IEEE International Conference on Micro Electro Mechanical Systems, Technical Digest, (2010), pp. 851–854.
[15] T. Thundat, L. Pinnaduwage, R. Lareau, Explosive vapour detection using micromechanical sensors, Electron. Noses Sens. Detect. Explos. 159 (2004) 249–266.
[16] G.M. Zuo, X.X. Li, Z.X. Zhang, et al., Dual-SAM functionalization on integrated cantilevers for specific trace-explosive sensing and non-specific adsorption suppression, Nanotechnology 18 (June (25)) (2007).
[17] M. Alvarez, L.G. Carrascosa, M. Moreno, et al., Nanomechanics of the formation of DNA self-assembled monolayers and hybridization on microcantilevers, Langmuir 20 (October (22)) (2004) 9663–9668.
[18] K.M. Hansen, H.F. Ji, G.H. Wu, et al., Cantilever-based optical deflection assay for discrimination of DNA single-nucleotide mismatches, Anal. Chem. 73 (April (7)) (2001) 1567–1571.
[19] K.S. Jin, S.R. Shin, B. Ahn, et al., pH-dependent structures of an i-motif DNA in solution, J. Phys. Chem. B 113 (February (7)) (2009) 1852–1856.
[20] K. Kang, M. Nilsen-Hamilton, P. Shrotriya, Differential surface stress sensor for detection of chemical and biological species, Appl. Phys. Lett. 93 (October (14)) (2008).
[21] K. Kang, M. Nilsen-Hamilton, P. Shrotriya, Novel differential surface stress sensor for detection of DNA hybridization, Proceedings of the ASME Summer Bioengineering Conference - 2009, Pt A and B, (2009), pp. 1159–1160.
[22] J.C. Stachowiak, M. Yue, K. Castelino, et al., Chemomechanics of surface stresses induced by DNA hybridization, Langmuir 22 (January (1)) (2006) 263–268.
[23] G.H. Wu, H.F. Ji, K. Hansen, et al., Origin of nanomechanical cantilever motion generated from biomolecular interactions, Proc. Natl. Acad. Sci. U. S. A. 98

(February (4)) (2001) 1560–1564.
[24] D. Lee, K.S. Hwang, S. Kim, et al., Rapid discrimination of DNA strands using an opto-calorimetric microcantilever sensor, Lab Chip 14 (24) (2014) 4659–4664.
[25] B. Ilic, D. Czaplewski, M. Zalalutdinov, et al., Single cell detection with micromechanical oscillators, J. Vac. Sci. Technol. B 19 (November–December (6)) (2001) 2825–2828.
[26] R. Raiteri, M. Grattarola, H.J. Butt, et al., Micromechanical cantilever-based biosensors, Sens. Actuators B: Chem. 79 (October (2–3)) (2001) 115–126.
[27] C.A. Savran, S.M. Knudsen, A.D. Ellington, et al., Micromechanical detection of proteins using aptamer-based receptor molecules, Anal. Chem. 76 (June (11)) (2004) 3194–3198.
[28] C. Li, G. Zhang, S. Wu, et al., Aptamer-based microcantilever-array biosensor for profenofos detection, Anal. Chim. Acta 1020 (2018) 116–122 2018/08/22/.
[29] M.F. Hagan, A. Majumdar, A.K. Chakraborty, Nanomechanical forces generated by surface grafted DNA, J. Phys. Chem. B 106 (October (39)) (2002) 10163–10173.
[30] L. Hood, J.R. Heath, M.E. Phelps, et al., Systems biology and new technologies enable predictive and preventative medicine, Science 306 (October (5696)) (2004) 640–643.
[31] L. Loo, J.A. Capobianco, W. Wu, et al., Highly sensitive detection of HER2 extracellular domain in the serum of breast cancer patients by piezoelectric microcantilevers, Anal. Chem. 83 (May (9)) (2011) 3392–3397.
[32] S. Sengupta, R. Sasisekharan, Exploiting nanotechnology to target cancer, Br. J. Cancer 96 (May (9)) (2007) 1315–1319.
[33] J. Mertens, C. Rogero, M. Calleja, et al., Label-free detection of DNA hybridization based on hydration-induced tension in nucleic acid films, Nat. Nanotechnol. 3 (May (5)) (2008) 301–307.
[34] H.H. Strey, V.A. Parsegian, R. Podgornik, Equation of state for polymer liquid crystals: theory and experiment, Phys. Rev. E 59 (January (1)) (1999) 999–1008.
[35] Z.-Q. Tan, Y.-C. Chen, N.-H. Zhang, Theoretical analysis for bending of single-stranded DNA adsorption on microcantilever sensors, Sensors 18 (9) (2018).
[36] A.R. Kadam, G.P. Nordin, M.A. George, Use of thermally induced higher order modes of a microcantilever for mercury vapor detection, J. Appl. Phys. 99 (May (9)) (2006).
[37] M. Su, V.P. Dravid, Surface combustion microengines based on photocatalytic oxidations of hydrocarbons at room temperature, Nano Lett. 5 (October (10)) (2005) 2023–2028.
[38] H.F. Ji, B.D. Armon, Approaches to increasing surface stress for improving signal-to-Noise ratio of microcantilever sensors, Anal. Chem. 82 (March (5)) (2010) 1634–1642.
[39] J. Zhang, H.P. Lang, F. Huber, et al., Rapid and label-free nanomechanical detection of biomarker transcripts in human RNA, Nat. Nanotechnol. 1 (December (3)) (2006) 214–220.
[40] C.M. Domínguez, P.M. Kosaka, G. Mokry, et al., Hydration induced stress on DNA monolayers grafted on microcantilevers, Langmuir 30 (36) (2014) 10962–10969 2014/09/16/.
[41] A. Gosai, B.S. Hau Yeah, M. Nilsen-Hamilton, et al., Label free thrombin detection in presence of high concentration of albumin using an aptamer-functionalized nanoporous membrane, Biosens. Bioelectron. (2018) 2018/10/18/.
[42] Y. Weizmann, F. Patolsky, O. Lioubashevski, et al., Magneto-mechanical detection of nucleic acids and telomerase activity in cancer cells, J. Am. Chem. Soc. 126 (February (4)) (2004) 1073–1080.
[43] H. Pei, N. Lu, Y.L. Wen, et al., A DNA nanostructure-based biomolecular probe carrier platform for electrochemical biosensing, Adv. Mater. 22 (November (42)) (2010) 4754–+.
[44] T. Hashimoto, X. Zhang, X. Zhou, et al., Investigation of dealloying of S phase (Al2CuMg) in AA 2024-T3 aluminium alloy using high resolution 2D and 3D electron imaging, Corros. Sci. 103 (February) (2016) 157–164.
[45] S.J. Culp, F.A. Beland, R.H. Heflich, et al., Mutagenicity and carcinogenicity in relation to DNA adduct formation in rats fed leucomalachite green, Mutat. Res. Mol. Mech. Mutagen. 506–507 (2002) 55–63 2002/09/30/.
[46] Q. Wang, X. Qin, L. Geng, et al., Label-free electrochemical aptasensor for sensitive detection of malachite green based on Au nanoparticle/graphene quantum dots/tungsten disulfide nanocomposites, Nanomaterials 9 (2) (2019).
[47] L. Wu, Z. Lin, H. Zhong, et al., Rapid determination of malachite green in water and fish using a fluorescent probe based on CdTe quantum dots coated with molecularly imprinted polymer, Sens. Actuators B: Chem. 239 (2017) 69–75.
[48] W. Xing, L. He, H. Yang, et al., Development of a sensitive and group-specific polyclonal antibody-based enzyme-linked immunosorbent assay (ELISA) for detection of malachite green and leucomalachite green in water and fish samples, J. Sci. Food Agric. 89 (13) (2009) 2165–2173 2009/10/01/.
[49] M. Vinchurkar, J. Phatak, V. R. Rao, etal., Polymeric piezoresistive-microcantilever based label-free malachite green biosensor: In situ detection of G-Quadruplex formation, 2016 IEEE International Nanoelectronics Conference (INEC), Chengdu, 2016, pp. 1-2.
[50] X. Feng, N. Gan, H. Zhang, et al., A novel "dual-potential" electrochemiluminescence aptasensor array using CdS quantum dots and luminol-gold nanoparticles as labels for simultaneous detection of malachite green and chloramphenicol, Biosens. Bioelectron. 74 (2015) 587–593 2015/12/15/.
[51] M. Ilgu, M. Nilsen-Hamilton, Aptamers in analytics, Analyst 141 (5) (2016) 1551–1568.
[52] T. Hianik, V. Ostatna, M. Sonlajtnerova, et al., Influence of ionic strength, pH and aptamer configuration for binding affinity to thrombin, Bioelectrochemistry 70 (January (1)) (2007) 127–133.
[53] A. Gosai, X. Ma, G. Balasubramanian, et al., Electrical stimulus controlled binding/unbinding of human thrombin-aptamer complex, Sci. Rep. 6 (2016) 37449 11/22/online.
[54] X. Ma, A. Gosai, G. Balasubramanian, et al., Aptamer based electrostatic-stimuli responsive surfaces for on-demand binding/unbinding of a specific ligand, J. Mater. Chem. B 5 (20) (2017) 3675–3685.
[55] V.S. Yerramilli, K.H. Kim, Labeling RNAs in live cells using malachite green aptamer scaffolds as fluorescent probes, ACS Synth. Biol. 7 (3) (2018) 758–766 2018/03/16/.
[56] T. Wang, J.A. Hoy, M.H. Lamm, et al., Computational and experimental analyses converge to reveal a coherent yet malleable aptamer structure that controls chemical reactivity, J. Am. Chem. Soc. 131 (41) (2009) 14747–14755 2009/10/21/.
[57] D.H. Nguyen, T. Dieckmann, M.E. Colvin, et al., Dynamics studies of a malachite green − RNA complex revealing the origin of the red-shift and energetic contributions of stacking interactions, J. Phys. Chem. B 108 (4) (2004) 1279–1286 2004/01/01/.
[58] T. Nguyen, R. Pei, D.W. Landry, et al., Label-free microfluidic characterization of temperature-dependent biomolecular interactions, Biomicrofluidics 5 (September (3)) (2011) 34118–341187.
[59] D. Grate, C. Wilson, Laser-mediated, site-specific inactivation of RNA transcripts, Proc. Natl. Acad. Sci. U. S. A. 96 (11) (1999) 6131.
[60] L. Zhai, T. Wang, K. Kang, et al., An RNA aptamer-based microcantilever sensor to detect the inflammatory marker, mouse lipocalin-2, Anal. Chem. 84 (October (20)) (2012) 8763–8770.
[61] K. Kang, M. Nilsen-Hamilton, P. Shrotriya, et al., Novel Differential Surface Stress Sensor for Detection of DNA Hybridization, (2009).
[62] T.M. Herne, M.J. Tarlov, Characterization of DNA probes immobilized on gold surfaces, J. Am. Chem. Soc. 119 (38) (1997) 8916–8920 1997/09/01/.
[63] R. Levicky, T.M. Herne, M.J. Tarlov, et al., Using self-assembly to control the structure of DNA monolayers on gold: a neutron reflectivity study, J. Am. Chem. Soc. 120 (38) (1998) 9787–9792 1998/09/01/.
[64] S.D. Keighley, P. Li, P. Estrela, et al., Optimization of DNA immobilization on gold electrodes for label-free detection by electrochemical impedance spectroscopy, Biosens. Bioelectron. 23 (8) (2008) 1291–1297 2008/03/14/.
[65] N. Bahner, P. Reich, D. Frense, et al., An aptamer-based biosensor for detection of doxorubicin by electrochemical impedance spectroscopy, Anal. Bioanal. Chem. 410 (5) (2018) 1453–1462 2018/02/01/.
[66] L.M. Demers, C.A. Mirkin, R.C. Mucic, et al., A fluorescence-based method for determining the surface coverage and hybridization efficiency of thiol-capped oligonucleotides bound to gold thin films and nanoparticles, Anal. Chem. 72 (22) (2000) 5535–5541 2000/11/01/.
[67] R. Karnik, K. Castelino, R. Fan, et al., Effects of biological reactions and modifications on conductance of nanofluidic channels, Nano Lett. 5 (9) (2005) 1638–1642 2005/09/01/.
[68] S. Nakano, D. Miyoshi, N. Sugimoto, Effects of molecular crowding on the structures, interactions, and functions of nucleic acids, Chem. Rev. 114 (5) (2014) 2733–2758 2014/03/12/.
[69] C. Daniel, Y. Roupioz, D. Gasparutto, et al., Solution-phase vs surface-phase aptamer-protein affinity from a label-free kinetic biosensor, PLoS One 8 (9) (2013) e75419.
[70] J. Flinders, S.C. DeFina, D.M. Brackett, et al., Recognition of planar and Nonplanar Ligands in the malachite green–RNA aptamer complex, ChemBioChem 5 (1) (2004) 62–72 2004/01/05/.
[71] G. Zhang, C. Li, S. Wu, et al., Label-free aptamer-based detection of microcystin-LR using a microcantilever array biosensor, Sens. Actuators B: Chem. 260 (2018) 42–47.
[72] J. Bernard Da Costa, T. Dieckmann, Entropy and Mg2+ control ligand affinity and specificity in the malachite green binding RNA aptamer, Mol. Biosyst. 7 (7) (2011) 2156–2163.
[73] S. Cai, J. Yan, H. Xiong, et al., Investigations on the interface of nucleic acid aptamers and binding targets, Analyst 143 (22) (2018) 5317–5338.
[74] K. Mitrowska, A. Posyniak, J. Zmudzki, Determination of malachite green and leucomalachite green residues in water using liquid chromatography with visible and fluorescence detection and confirmation by tandem mass spectrometry, J. Chromatogr. A 1207 (1) (2008) 94–100 2008/10/17/.
[75] Y. Zhang, W. Yu, L. Pei, et al., Rapid analysis of malachite green and leucomalachite green in fish muscles with surface-enhanced resonance Raman scattering, Food Chem. 169 (2015) 80–84 2015/02/15/.
[76] J. Hou, F. Bei, M. Wang, et al., Electrochemical determination of malachite green at graphene quantum dots–gold nanoparticles multilayers–modified glassy carbon electrode, J Appl Electrochem 43 (7) (2013) 689–696.
[77] H. Dai, L. Gong, G. Xu, et al., An electrochemical sensing platform structured with carbon nanohorns for detecting some food borne contaminants, Electrochimica Acta 111 (2013) 57–63.

Yue Zhao received his PhD from Iowa State University on 2014. His thesis topic is on surface stress detection and mechanism study with microcantilever based sensor for biomolecular monolayers. Yue has multiple publications on aptamer based microcantilever sensors.

Agnivo Gosai received his PhD from Iowa State University on 2018. He has worked on aptamer based sensors for portable diagnostics towards human disease detection. His thesis deals with the engineering of nano-bio interfaces of sensor transducers towards improved performance of devices.

Pranav Shrotriya is a professor at the Mechanical Engineering department of Iowa State University, Ames, Iowa, USA. He is the recipient of NSF career award on "High Resolution Interferometry Based Surface Stress Sensors for Chemical and Biological Species Detection" and has extensive experience on laser interferometer based microcantilever biosensors as well as electrochemical sensors.